Principle of Magnetic Force Microscopy

Leon Abelmann

Systems and Materials for Information Storage
University of Twente, The Netherlands

July 27, 2005

The technique of Magnetic Force Microscopy has been discussed extensively in literature [3, 5, 4], so we will restrict ourselves to a short description. The principle of Magnetic Force Microscopy is very much like that of Atomic Force Microscopy – some even dare to mention that *MFM is just an AFM with a magnetic tip*, much to the dislike of MFM developers because in an MFM much smaller forces are measured. In essence it is true however, and every MFM is capable of AFM as well (the other way round is not true in general).

In an MFM the magnetic stray field above a very flat specimen, or sample, is detected by placing a small magnetic element, the tip, mounted on a cantilever spring very close to the surface of the sample (figure 1). Typical dimensions are a cantilever length of 200 μm , tip length of 4 μm and diameter of 50 nm and a distance from the surface of 30 nm. The force on the magnetic tip is detected by measuring the displacement of the end of the cantilever, usually by optical means. The forces measured in typical MFM applications are in the order of 30 pN, with typical cantilever deflections on the order of nanometers.

An image of the magnetic stray field is obtained by slowly scanning the cantilever over the sample surface, in a raster-like fashion. Typical scan areas are from 1 up to 200 μm with imaging times in the order of 5-30 minutes.

1 Mode of operation

The force F excerted on the tip by the stray field of the sample has two effects on the cantilever deflection. In the first place the cantilever end is deflected towards or away from the sample surface by a distance Δz:

$$\Delta z = F_z/c \quad [m] \tag{1}$$

Where c is the cantilever spring constant in z-direction $[N/m]$. This deflection can be measured using soft, usually Si_3N_4 , cantilevers with spring constants in the order of 0.01-0.1 N/m. When measuring the deflection, we speak about *static mode* MFM .

For small deflections, the cantilever can be considered as a damped harmonic oscillator, which can be modelled by an ideal spring c $[N/m]$, mass m $[kg]$ and damper D $[Ns/m]$ [2]. When we apply an external oscillating force $F_z = F_0 cos(\omega t)$ to the cantilever, the resulting displacement is harmonic as well, but has a phase shift for $\omega > 0$, $z = z_0 cos(\omega t + \theta(\omega))$. This force can be applied directly to the end of the cantilever, for instance by electrostatic means. To most commonly used method is however to apply a force to the cantilever holder, by means of a piezo mounted underneath the holder.

It is convenient to desribe the relation between force and displacement in the Laplace domain [1]

[1] We use the definition commonly used in mechanical engineering textbooks $\widehat{F}(s) = \int_{-\infty}^{+\infty} f(t)e^{-st}dt$

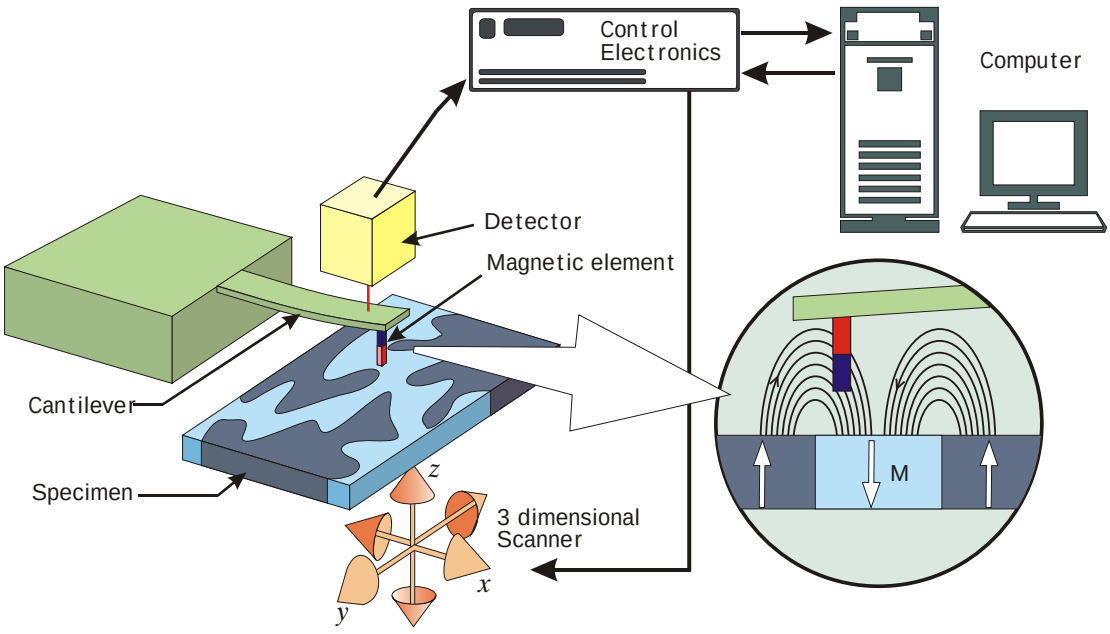

Figure 1: Principle of Magnetic Force Microscopy

$$\frac{\widehat{Z}}{\widehat{F}} = \frac{1}{c + sD + ms^2} \quad [m/N] \tag{2}$$

Using the natural resonance frequency ω_n and unitless damping factor δ

$$\omega_n = \sqrt{c/m} \quad [2\pi/s] \tag{3}$$

$$\delta = \frac{D}{2\sqrt{mc}} = \frac{D\omega_n}{2c} \tag{4}$$

we can rewrite (2) into

$$\frac{\widehat{Z}}{\widehat{F}} = \frac{1}{m\omega_n^2 + 2\delta\omega_n ms + ms^2} \quad [m/N] \tag{5}$$

For underdamped systems ($\delta < 1$), this system has poles at

$$s_{1,2} = -\delta\omega_n \pm i\omega_n\sqrt{1-\delta^2} = -\delta\omega_n \pm i\omega_d \tag{6}$$

The term $\omega_d = \omega_n\sqrt{1-\delta^2}$ is referred to as the *damped natural frequency*. For MFM in dynamic mode cantilevers with very small damping ($\delta \ll 0.01$) are used and $\omega_d \approx \omega_n$. In MFM it is custom to talk about the *quality factor* of resonance Q, instead of the damping factor. Q is proportional to the ratio between the energy stored in the cantilever and the energy lost per cycle:

$$Q = 2\pi\frac{\text{Energy stored in cantilever}}{\text{Energy lost per cycle}} = 2\pi\frac{\frac{1}{2}cz_0^2}{\pi D z_0^2\omega_n} = \frac{c}{D\omega_n} = \frac{1}{2\delta} \tag{7}$$

Using Q (5) becomes:

$$\frac{\widehat{Z}}{\widehat{F}} = \frac{1}{m\omega_n^2 + \frac{\omega_n m}{Q}s + ms^2} \quad [m/N] \tag{8}$$

From (8) we can calculate the amplitude z_0 of the cantilever vibration when driven at a frequency ω [1]

$$z_0 = \frac{F_0/m}{\sqrt{(\omega_n^2 - \omega^2)^2 + (\omega\omega_n/Q)^2}} \tag{9}$$

and the phase shift θ between the force and the deflection (Also see figure 2)

$$\theta = \tan^{-1}\left(\frac{\omega\omega_n}{Q(\omega_n^2 - \omega^2)}\right) \tag{10}$$

In MFM, the force on the magnetic tip increases when it approaches the sample, so it is as if there is a second spring with a spring constant of $\partial F/\partial z$ attached to the cantilever. In the case that the cantilever deflection so small that $\partial F/\partial z$ can be considered a constant, this results in a change in natural resonance frequency $f_n = \omega_n/2\pi$ of the cantilever

$$f_n' = f_n\sqrt{1 - \frac{\partial F_z/\partial z}{c}} \quad [Hz] \tag{11}$$

$$\Delta f = f_n' - f_n \approx -\frac{f_n}{2c}\frac{\partial F_z}{\partial z} \quad [Hz] \tag{12}$$

The approximation is accurate for $\Delta f \ll f_n$, which is always the case in MFM. Note the sign of Δf. In the above equations it is assumed that the positive z-direction is pointing away from the surface. When the tip is attracted towards the sample, the force therefore is *negative*, and the force derivative is positive. So for *attracting* forces the resonance frequency of the cantilever *decreases*. Please note that expression (11) is only valid for small vibration amplitudes. When $\partial F/\partial z$ cannot be considered constant, the vibration contains higher harmonics and more elaborate, and even numerical methods are needed to calculate the resonance frequency shifts.

When we measure the resonance frequency of the cantilever, we speak about *dynamic* mode MFM (indicated by *frequency* in fig 2). In this mode the cantilever is usually forced to resonate at an amplitude of 10-30 nm, so that an accurate detection of the very small frequency shifts is possible (typically 3 Hz on 80 kHz). In this mode a control circuit is needed which

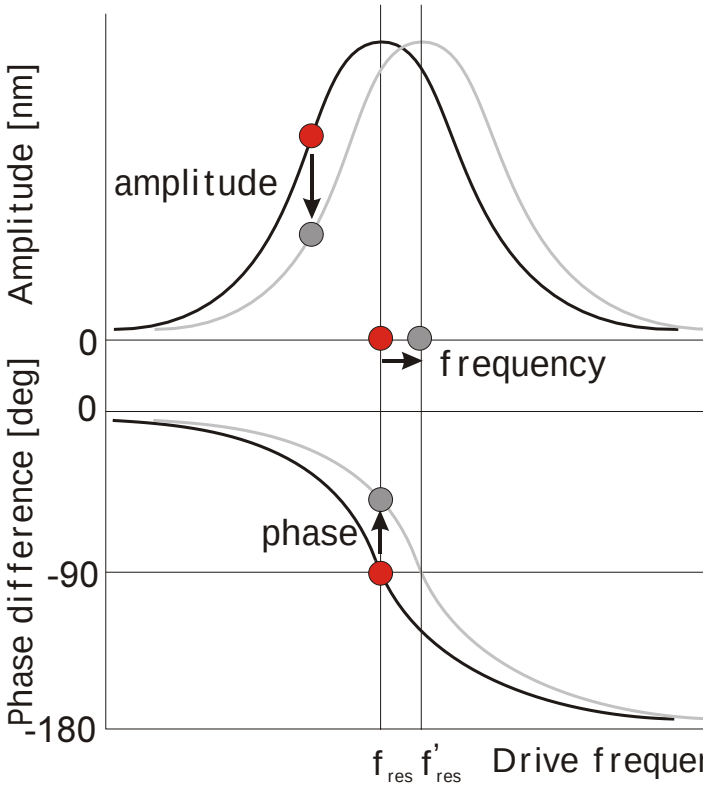

Figure 2: A change of the magnetic force on the tip results in a change in resonance frequency of the cantilever, which can be detected in different ways.

matches the beat frequency of the actuator that drives the cantilever (e.g. a piezo), with the actual resonance frequency. Very often a phase locked loop (PLL) circuit is used, which keeps the phase difference between the driving signal and the measured deflection of the cantilever at approximately 90^o. This control circuit adds additional noise to the measurement signal. For small signals it is therefore sometimes preferable to fix the frequency of the driving signal to f_n and measure the phase difference between the driving signal and the measured cantilever deflection (indicated by *phase* in fig 2). The phase shift, which is in the order of a few degrees, strongly depends on the damping of the cantilever, which on its turn is a function of many parameters. The phase signal is therefore not really suitable for quantitative analysis.

An even simpler dynamic detection mode is to drive the cantilever off-resonance. A change in resonance frequency will result in change of the vibration amplitude (*amplitude* in fig 2). Even though this amplitude mode works fine for AFM, it gives very poor results for MFM because the amplitude variations are small compared to the noise. Moreover the response of the cantilever to a change in force is slow when the quality factor of resonance is high, which is for instance the case in vacuum[1]. Therefore this mode is not used very often.

Fundamentally there is no difference in sensitivity between the static mode and dynamic mode, because both modes use the same measurement geometry. For a number of reasons, to which we will come back later, the dynamic mode often gives better results however.

2 Image formation

To calculate the force on the magnetic tip, we have to start with the calculation of the energy U of the tip/sample system. The gradient of this energy then gives us the force vector. For MFM we are particularly interested in $\partial U/\partial z$.

We have two ways to calculate U . One can either calculate the energy of the magnetic tip in presence of the sample stray field or the energy of the magnetic sample in presence of the tip stray field[4]. In both cases we have to integrate the inner product of magnetic field and magnetization over the area where the magnetization is not zero:

$$U = -\mu_0 \int_{tip} \vec{M}_{tip}\vec{H}_{sample}dV = -\mu_0 \int_{sample} \vec{M}_{sample}\vec{H}_{tip}dV \tag{13}$$

Which method is more convenient, depends on the problem which is to be analysed. One usually takes that form for which the stray field calculation is more easy to perform.

When discussing image formation and resolution, it is convenient to do that in the spatial frequency domain- a method commonly used in magnetic recording theory. We therefore decompose the sample magnetization $\vec{M}$ in the sample plane (x, y) into their Fourier components, leaving the z component untransformed:

$$\vec{\tilde{M}}(k_x, k_y, z) = \int_{-\infty}^{\infty}\int_{-\infty}^{\infty} \vec{M}(x, y, z)e^{-i(xk_x+yk_y)}dxdy \tag{14}$$

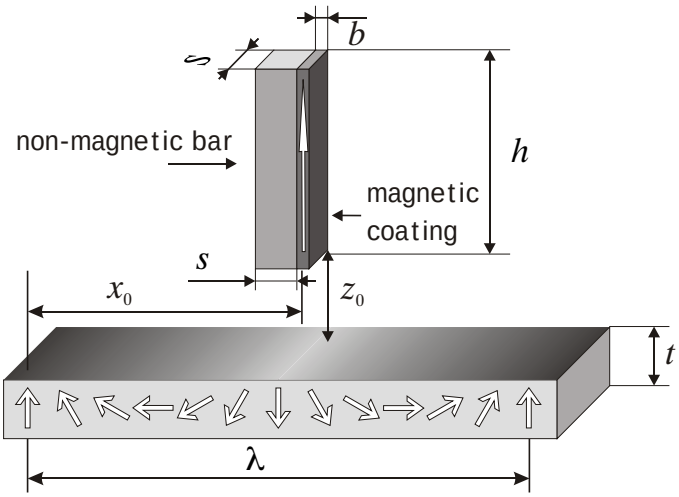

Figure 3: The ideal MFM tip has a bar shape and a magnetization fixed along its axis

The relation between the wavelength of a certain component λ and the Fourier components is

$$\vec{k} = (k_x, k_y) \tag{15}$$

$$k_{x(y)} = \frac{2\pi}{\lambda_{x(y)}} \tag{16}$$

The stray field of the sample generated by this magnetization distribution can be calculated by means of a Laplace transform. For a thin film with thickness t one can obtain with some patience [7]

$$\begin{pmatrix} \widehat{H}_x(k_x,k_y,z) \\ \widehat{H}_y(k_x,k_y,z) \\ \widehat{H}_z(k_x,k_y,z) \end{pmatrix} = \begin{pmatrix} -ik_x/|\vec{k}| \\ -ik_y/|\vec{k}| \\ 1 \end{pmatrix} \frac{1}{2}(1-e^{-|\vec{k}|t})e^{-|\vec{k}|z}\widehat{\sigma}_{eff}(\vec{k}) \tag{17}$$

Where $\widehat{\sigma}_{eff}(\vec{k})$ is an *effective* surface charge distribution. It expresses the property of the Laplace transformation that the stray field at height z above the sample surface is fully determined by the stray field at height $z = 0$. The effective surface charge distribution can be seen as a sheet of charges at the sample surfaces, which causes the same stray field as the more complex charge distribution within the sample itself[2].

For a sample with perpendicular magnetization ($M_x = 0, M_y = 0$), $\sigma_{eff}(x, y)$ simply equals the surface charge density σ.

$$\widehat{\sigma}_{eff}(\vec{k}) = \widehat{M_z}(\vec{k}) = \widehat{\sigma}(\vec{k}) \tag{18}$$

For a sample with an in-plane magnetization (so $M_z = 0$) we only have volume charges $\rho(x, y)$. If the magnetization is constant over the film thickness ($\partial M_x/\partial z = 0, \partial M_y/\partial z = 0$) the effective surface charge distribution becomes

$$\widehat{\sigma}_{eff}(\vec{k}) = -\frac{i\vec{k}}{|\vec{k}|} \cdot \vec{\widehat{M}}(\vec{k}) = \frac{\widehat{\rho}(\vec{k})}{|\vec{k}|} \tag{19}$$

For more complex situations, every magnetic charge in the sample has to be transformed, which results in rather lengthly expressions, and this method looses its power. In that case it might be easier to calculate the stray field from the tip.

Assuming a known effective surface charge distribution, we can now calculate the energy of the tip/sample system by combining (13) and (17). The only thing left unknown is the magnetization distribution in the MFM tip, which can be very complex. We will restrict ourselves however to the bar type tip with a magnetization fixed along the z-axis (Figure 3), in the first place because this is the ideal MFM tip shape [6] and in the second place because it results in very illustrative closed-form equations. The procedure to obtain the force F_z involves a simple integral of the stray field over the recangular tip volume, and taking $\partial U/\partial z$[6]:

$$\begin{aligned} \widehat{F}_z(\vec{k},z) = &-\mu_0 M_t \cdot b\, sinc(\frac{k_x b}{2}) \cdot S\, sinc(\frac{k_y S}{2}) \\ &\times(1-e^{-|\vec{k}|h})(1-e^{-|\vec{k}|t})e^{-|\vec{k}|z}\widehat{\sigma}_{eff}(\vec{k}) \end{aligned} \tag{20}$$

[2]The $\widehat{\sigma}_{eff}$ introduced here differs by a factor of 2 from the effective surface charge distribution defined in [7, 6]

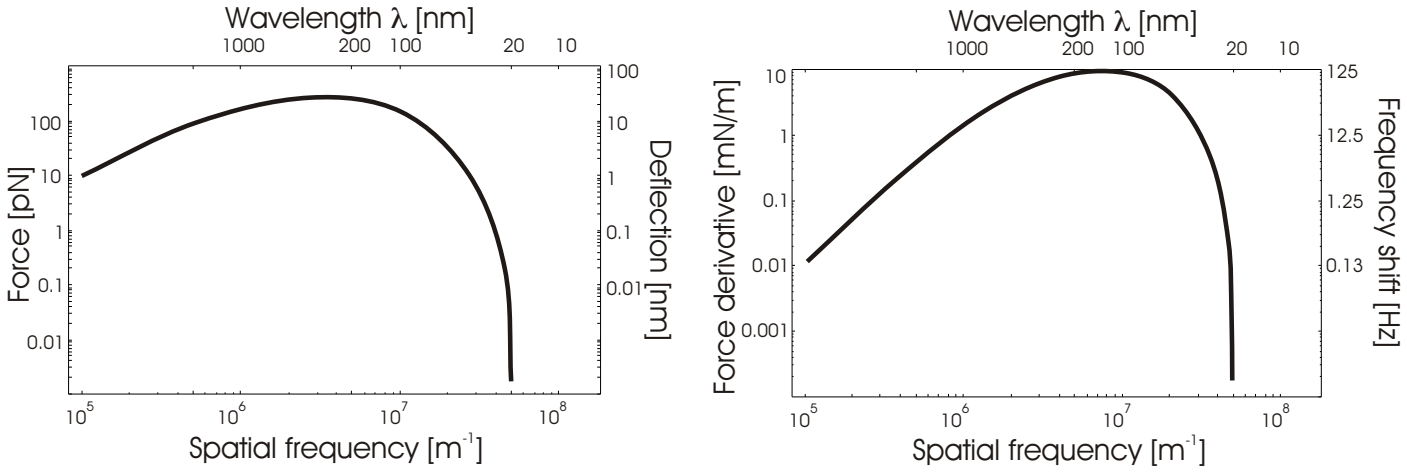

Figure 4: Tip transfer functions for a typical situation (table 1)

Where M_t is the tip magnetization $[A/m]$, $b \times S$ the tip cross section, h the tip height, t the film thickness and z the tip/sample distance (all in $[m]$)[3]. This relation between the force and the effective surface magnetization is often called the *tip transfer function* (TTF).

Allthough (20) is complex, it is not difficult to understand. We see that the force is proportional to the tip magnetization and the magnetic charge density (σ) in the sample, combined with a number of geometrical loss factors. For most situations in magnetic data storage research, the films under investigation are thin and the film thickness loss term $(1 - e^{-|\vec{k}|t})$ will dominate over the tip height term $(1 - e^{-|\vec{k}|h})$. If we further assume that the tip cross-section $(b \times S)$ is much smaller than the smallest features of the charge distribution in the film, we get a very simple expression for the TTF

$$\widehat{F}_z(\vec{k}, z) = -\mu_0 M_t b S (1 - e^{-|\vec{k}|t}) e^{-|\vec{k}|z} \widehat{\sigma}_{eff}(\vec{k}) \tag{21}$$

This approximation can be called the *monopole* approximation, because we assume that all magnetic charges ($M_t bS$) are located at one point at the end of the tip, and that the other charges are very far away from the sample surface. The only loss terms that remain are the film thickness loss, and the tip-sample distance loss, which usually is dominant. This immediately shows that for a good signal to noise ratio (SNR) in the image, the tip/sample distance has to be as small as possible.

When the details in the image start to approach the tip dimensions, the *sinc* functions have to be considered as well. For this bar type tip, the force becomes zero when the wavelength of the surface charge distribution equals the tip size. This is analogue to the situation in magnetic recording, where at the *gap zero* the bitsize is half the gap-size of the recording head.

The force we calculate in (20) is measured by means of a cantilever deflection or change in resonance frequency. For the latter case $\partial F_z / \partial z$ has to be calculated, which in the Fourier domain is simply:

$$\frac{\partial \widehat{F}_z(\vec{k}, z)}{\partial z} = -|\vec{k}| \widehat{F}_z(\vec{k}, z) \tag{22}$$

A typical example of TTFs for the static and dynamic mode and the resulting deflection and resonance shift, calculated from (1) and (12), is given in figure 4. In this case we consider a sample with perpendicular magnetization and only magnetic surface charges, using the parameters from table 1.

M_t	Tip magnetization	1422 kA/m
b	Tip thickness (coating thickness)	20 nm
s	Tip width	100 nm
h	Tip length	1 μm
M_s	Sample saturation magnetization	295 kA/m
t	Sample thickness	70 nm
z_0	Tip sample distance	20 nm
c	Cantilever spring constant	0.01 (3) N/m
f_n	Cantilever resonance frequency	7 (75) kHz

Table 1: Parameters used to calculate the tip transfer functions shown in figure 4. Values in parentheses are for the dynamic mode curves

[3] $sinc(x) = sin(x)/x$

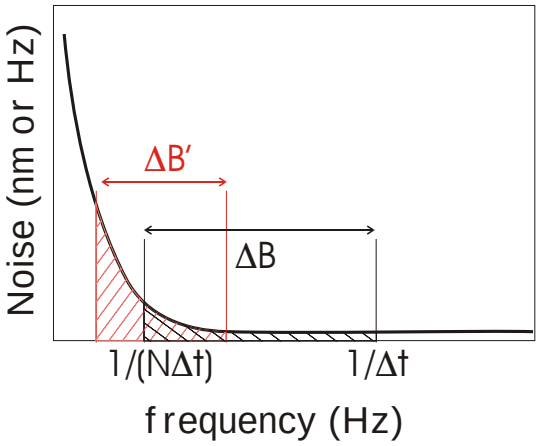

Figure 5: Increasing the measurement time can increase low frequency noise

3 Critical wavelength

Although everyone knows what a high resolution image is, to quantify resolution is not trivial. When an imaging system has high resolution, we usually mean that it is able to separate two closely spaced objects. We do not mean that it can detect one single small object: this has to do with sensitivity. We can define resolution as the minumum spacing between two objects that can still be observed. Instead of two, we can of course take a number of equally closed spaced objects. If we take an array, we can even define resolution in a certain direction. By using the array, the definition of resolution can quite naturally be transferred to the spatial frequency domain as the *minimum spacial wavelength that can still be observed*. Using the theory of section 2, we see that the signal strongly decreases for high frequency components, or small wavelengths. Analog to magnetic recording theory, we can define a certain upper limit on the spatial frequency, above which we call the signal 'non-detectable'. This is usually done with respect to the background noise level: the signal to noise ratio (SNR) should exceed a certain value. For magnetic recording, the SNR should be about a factor of 10 (20 dB), for imaging we consider an image still acceptable at an SNR as low as 2 (3 dB).

In principle, the SNR can be made arbitrarily high by increasing the measurement time, because that decreases the measurement bandwidth. This however assumes that the background noise is white, i.e. it has a flat frequency spectrum. In practice, the noise strongly increase when the frequency becomes very low. This is usually referred to as $1/f$ noise and is caused by drift, for instance by temperature variations or piezo creep. As an illustration, let us take the schematic noise spectrum of figure 5. The measurement bandwidth ΔB is related to the measurement time between the pixels Δt and the total number of pixels N, the combination of which determines the total time to measure an image.

$$\Delta B = \frac{1}{\Delta t} - \frac{1}{N\Delta t} \approx \frac{1}{\Delta t} \tag{23}$$

We see that the bandwidth is inversely proportional to the measurement time. But at long measurement times, the bottom of the measurement band will enter the $1/f$ noise region, which is indicated by $\Delta B'$ in figure 5. So if we exceed a certain measurement time, the total noise (there area under the curve) will start to increase, and cancel out the effect of a smaller bandwidth. In MFM, this situation results in a 'stripy' image, where the individual scanlines have noticeable offsets with respect to each other. Image processing can partly eliminate this effect (remove line average), but only if the low frequency noise periods are much longer than the time between scanlines. (One should be careful however, because with imaging processing of this kind one enters the twilight zone of image manipulation). So for reasons of image quality, and of course for practical reasons, we always have to take a limited measurement time into account. A minumum bandwidth of 200 Hz is reasonable. This allows us to link noise in the frequency domain to noise in the spatial domain through the scanspeed. Now we can find the resolution in figures like figure 6, by calculating the wavelength where the signal drops below the noise level multiplied with the desired SNR. Because the minumum SNR is quite low and usually the tip transfer function is very steep around this point, we simply set the SNR to unity. We call this point the *critical wavelength* or λ_c.

References

[1] T. R. Albrecht, P. Grutter, D. Horne, and D. Rugar. Frequency modulation detection using high-q cantilevers for enhanced force microscope sensitivity. *J Appl Phys*, 69(2):668–673, 1991. 2, 3

[2] D.K. Anand. *Introduction to Control Systems*. Pergamon Press, Oxford, 2 edition, 1984. 1

[3] P. Grütter, H.J. Mamin, and D. Rugar. Magnetic force microscopy. In H.J. Günterrodt and R. Wiesendanger, editors, *Scanning Tunneling Microscopy*, volume II, pages 151–207. Springer, Berlin, Heidelberg, New York, 1992. 1

[4] A[lex] Hubert and R[udi] Schäfer. *Magnetic domains: the analysis of magnetic microstructures*. Springer-Verlag, Berlin, Heidelberg, New-York, 1998. 1, 3

[5] S. Porthun, L. Abelmann, and C. Lodder. Magnetic force microscopy of thin film media for high density magnetic recording. *Journal of Magnetims and Magnetic Materials*, 182(1-2):238–273, 1998. 1

[6] S. Porthun, L. Abelmann, S. J. L. Vellekoop, J. C. Lodder, and H. J. Hug. Optimization of lateral resolution in magnetic force microscopy. *Applied Physics A- Mate Sci Process*, 66(Suppl. Part 2):S1185–S1189, 1998. 4

[7] B. Vellekoop, E. Abelmann, S. Porthun, and C. Lodder. On the determination of the internal magnetic structure by magnetic force microscopy. *J Magn Magn Mater*, 190(1-2):148–151, 1998. 4

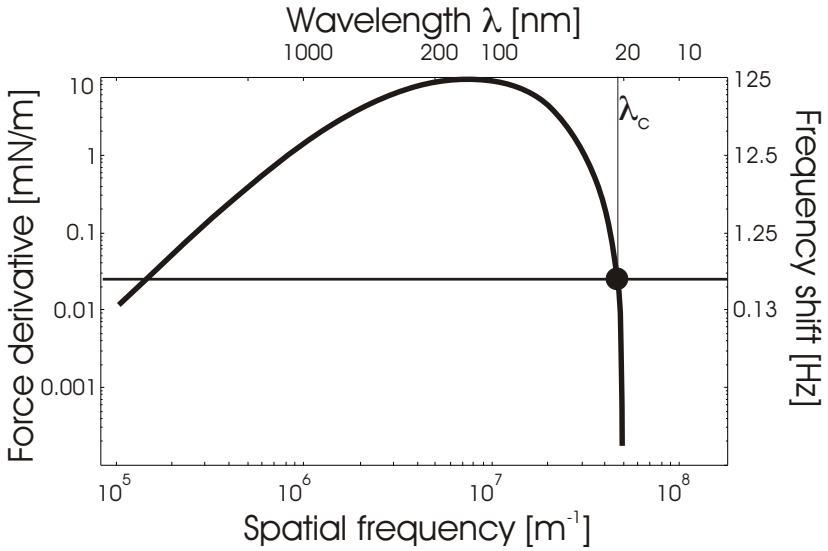

Figure 6: Using the background noise level, we can define the limit of resolution by means of a critical wavelength (λ_c)